ELSEVIER

Journal of Power Sources 81–82 (1999) 90–94

JOURNAL OF POWER SOURCES

www.elsevier.com/locate/jpowsour

Solid-state redox potentials for $Li[Me_{1/2}Mn_{3/2}]O_4$ (Me: 3d-transition metal) having spinel-framework structures: a series of 5 volt materials for advanced lithium-ion batteries

Tsutomu Ohzuku *, Sachio Takeda, Masato Iwanaga

Electrochemistry and Inorganic Chemistry Laboratory, Department of Applied Chemistry, Faculty of Engineering, Osaka City University, Sugimoto 3-3-138, Sumiyoshi, Osaka, 558-8585, Japan

Abstract

A series of spinel-framework structures of $Li[Me_{1/2}Mn_{3/2}]O_4$ (Me; Ti, Cr, Fe, Co, Ni, Cu, and Zn) was prepared and examined by XRD and electrochemical methods. All samples except $Li[Ti_{1/2}Mn_{3/2}]O_4$ and $Li[Zn_{1/2}Mn_{3/2}]O_4$ exhibited approximately 5 V solid-state redox potentials (vs. Li^+/Li), probably due mainly to compact crystal fields imposed by the spinel-framework structure of cubic close-packed oxygen linked with tetravalent manganese ions. Of these, $Li[Fe_{1/2}Mn_{3/2}]O_4$ and $Li[Ni_{1/2}Mn_{3/2}]O_4$ are very attractive materials in both basic and applied research fields, and the solid-state redox potentials of transition metal ions in such crystal fields are summarized and discussed.

Keywords: Solid-state redox potentials; $Li[Me_{1/2}Mn_{3/2}]O_4$; Lithium-ion batteries

1. Introduction

A spinel-framework structure with lithium, manganese and oxygen shows a unique character such that manganese ions ($3d^3$ or $3d^4$) at the octahedral 16(d) sites in the space group Fd3m can be replaced easily by lithium ions ($2s^0$) without the dramatic structural changes (as determined by XRD [1]) while conserving net charge, giving anomalous non-stoichiometric characteristics. Manganese ions at the 16(d) sites can also be replaced by other transition metal ions [2]. Transition metal ions other than manganese in such a spinel-framework structure are exposed to a quite different environment compared with the self-assembled lithiated metal oxide of their own kind. Therefore, we can expect anomalous solid-state redox potentials for transition metal ions in this structure, and we carried out a series of experimental and theoretical studies to determine the solid-state electrochemistry of these lithium insertion materials for advanced lithium batteries. This paper describes our preliminary results.

2. Experimental

$Li[Me_{1/2}Mn_{3/2}]O_4$ (Me; Ti, Cr, Fe, Co, Ni, Cu, and Zn) were prepared by combining LiOH, MnOOH (manganite), TiO_2 (anatase), Cr_2O_3, FeOOH (goethite), $Co(OH)_2$, $Ni(OH)_2$, CuO, or $Zn(OH)_2$. Reaction mixtures (Li:Me:Mn = 2:1:3 in molar ratio) were typically pressed into pellets (23 mm dia. and ca. 5 mm thick.) and heated at 550°C in air or oxygen for 15 h. These pre-calcined materials were then ground and again pressed into pellets, which were subsequently reacted at 750°C in air or oxygen for 15 h. The final reaction product was ground and characterized by XRD. The samples were stored in a desiccator over blue silica-gel before use.

To prepare electrodes for electrochemical tests, 80 wt.% of sample, 10 wt.% acetylene black, and 10 wt.% polyvinylidene fluoride (PVDF) dissolved in *N*-methyl-2-pyrrolidone (NMP) solution was painted onto aluminum sheets (15×20 mm^2) and then dried under vacuum at 150°C for 12 h. Two sheets of porous membrane (Celgard 2500) were used as a separator, and the electrolyte was 1 M

* Corresponding author

0378-7753/99/$ - see front matter
PII: S0378-7753(99)00246-3

$LiPF_6$ dissolved in ethylene carbonate (EC)/diethyl carbonate (DEC) (1/1 by volume). The electrochemical cells and data acquisition systems were the same as described previously [3,4].

3. Results and discussion

Fig. 1 shows the X-ray diffraction (XRD) patterns of a series of $Li[Me_{1/2}Mn_{3/2}]O_4$ (Me;Ti, Cr, Fe, Co, Ni, Cu, and Zn) powders. In Fig. 1, $LiMn_2O_4$ is also shown in comparison. All diffraction lines can be indexed by comparing with those of $LiMn_2O_4$ [5]. Because the lattice parameters of $Li[Li_xMn_{2-x}]O_4$ $(0 \leq x < 1/3)$ fall in the range $a = 8.16$–8.24 Å [1], our results suggest that the transition metal ions are located primarily at the octahedral 16(d) sites in the space group Fd3m, and the lattice dimension is mainly determined by a spinel-framework based on manganese and oxygen ions. The (2,2,0) line in $Li[Zn_{1/2}Mn_{3/2}]O_4$ suggests that a part of zinc ions is located at the 8(a) sites in this case. Of these, only $Li[Ti_{1/2}Mn_{3/2}]O_4$ ($a = 8.33$ Å) and $Li[Fe_{1/2}Mn_{3/2}]O_4$ ($a = 8.27$ Å) have lattice dimensions larger than that of $LiMn_2O_4$ ($a = 8.24$ Å).

The results of slow-scan voltammetry are shown in Fig. 2. Electrochemical behaviors of $Li[Cr_{1/2}Mn_{3/2}]O_4$ [6], $Li[Ni_{1/2}Mn_{3/2}]O_4$ [7], and $Li[Cu_{1/2}Mn_{3/2}]O_4$ [8,9] in nonaqueous lithium cells have already been reported as 5 V materials for lithium-ion batteries. Our data are consistent with these prior results in terms of their high-voltage characteristics in nonaqueous lithium batteries. As can be seen in Fig. 2, the chromium, iron, cobalt, nickel, or copper-containing sample having a spinel-framework structure based on lithium, manganese, and oxygen gives operating voltage higher than 4.5 V in addition to normal operating voltage around 4.0 V observed for $LiMn_2O_4$ (more generally $Li[Li_xMn_{2-x}]O_4$ $(0 \leq x < 1/3)$ [1,10]). Of these, $Li[Ni_{1/2}Mn_{3/2}]O_4$ appears differently when it compares with other materials. This is better illustrated in charge and discharge curves shown in Fig. 3. $Li[Ni_{1/2}Mn_{3/2}]O_4$ shows predominantly one-step reaction at 4.8 V while other materials shows approximately two-step reactions at 4.0 V and ca. 5 V. The charge and discharge curve for $Li[Cr_{1/2}Mn_{3/2}]O_4$ looks quite similar to that for $Li[Fe_{1/2}Mn_{3/2}]O_4$. One cannot tell which is which from the charge and discharge curves. In Fig. 3, we adopted first charge and discharge curves. The loss of capacity during the first charge and discharge is in the following order: $Ni < Cr \approx Cu < Fe < Co$, which is the same as that in operating voltage order. This indicates that the loss of capacity is mainly due to electrolyte decomposition which occurs above 4.8 V. Longer stay of the electrodes at higher voltage gives larger loss of capacity.

Although some obscurity exists in the electrochemical results, we tentatively formulate electrochemical reactions of these materials to calculate theoretical capacity for

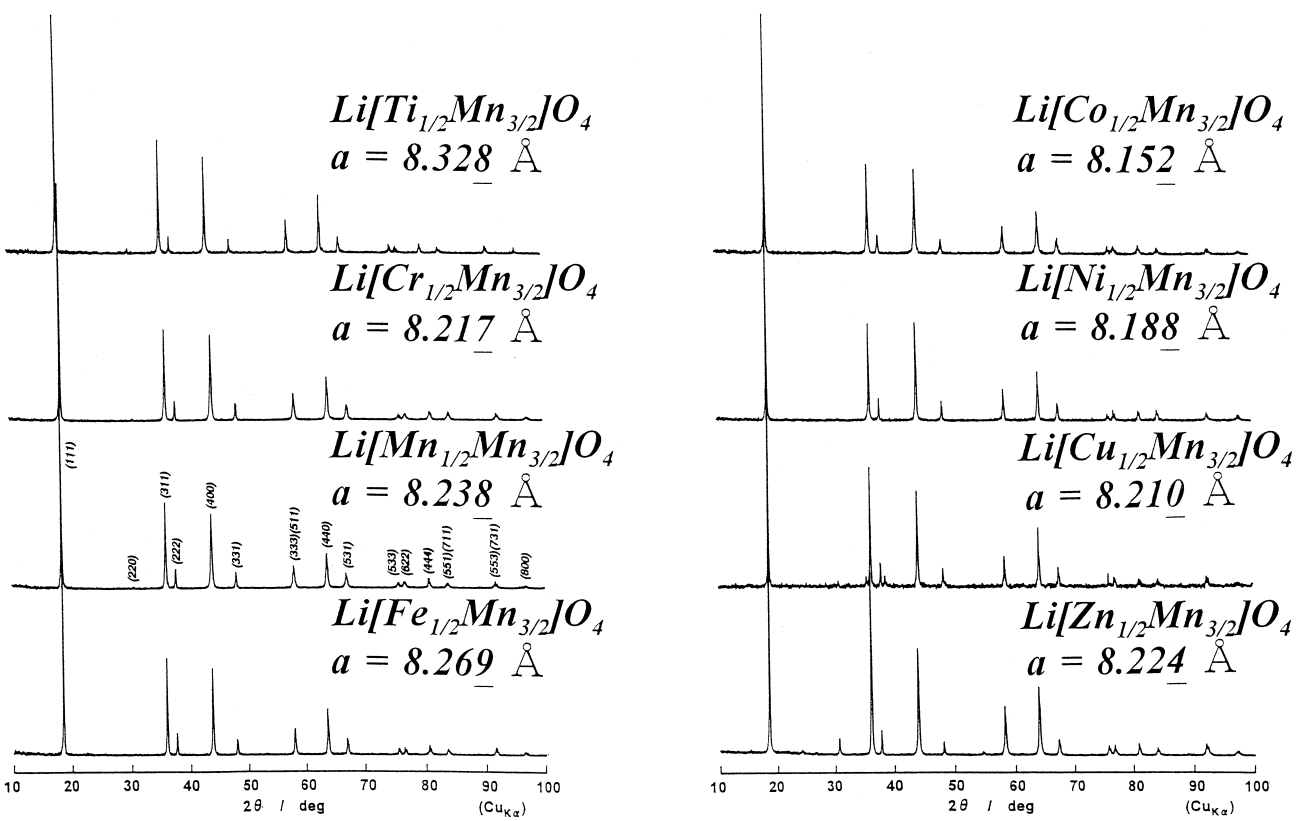

Fig. 1. X-ray diffraction patterns of $Li[Me_{1/2}Mn_{3/2}]O_4$ (Me:Ti, Cr, Fe, Co, Ni, Cu, and Zn). $LiMn_2O_4$ is also shown in comparison.

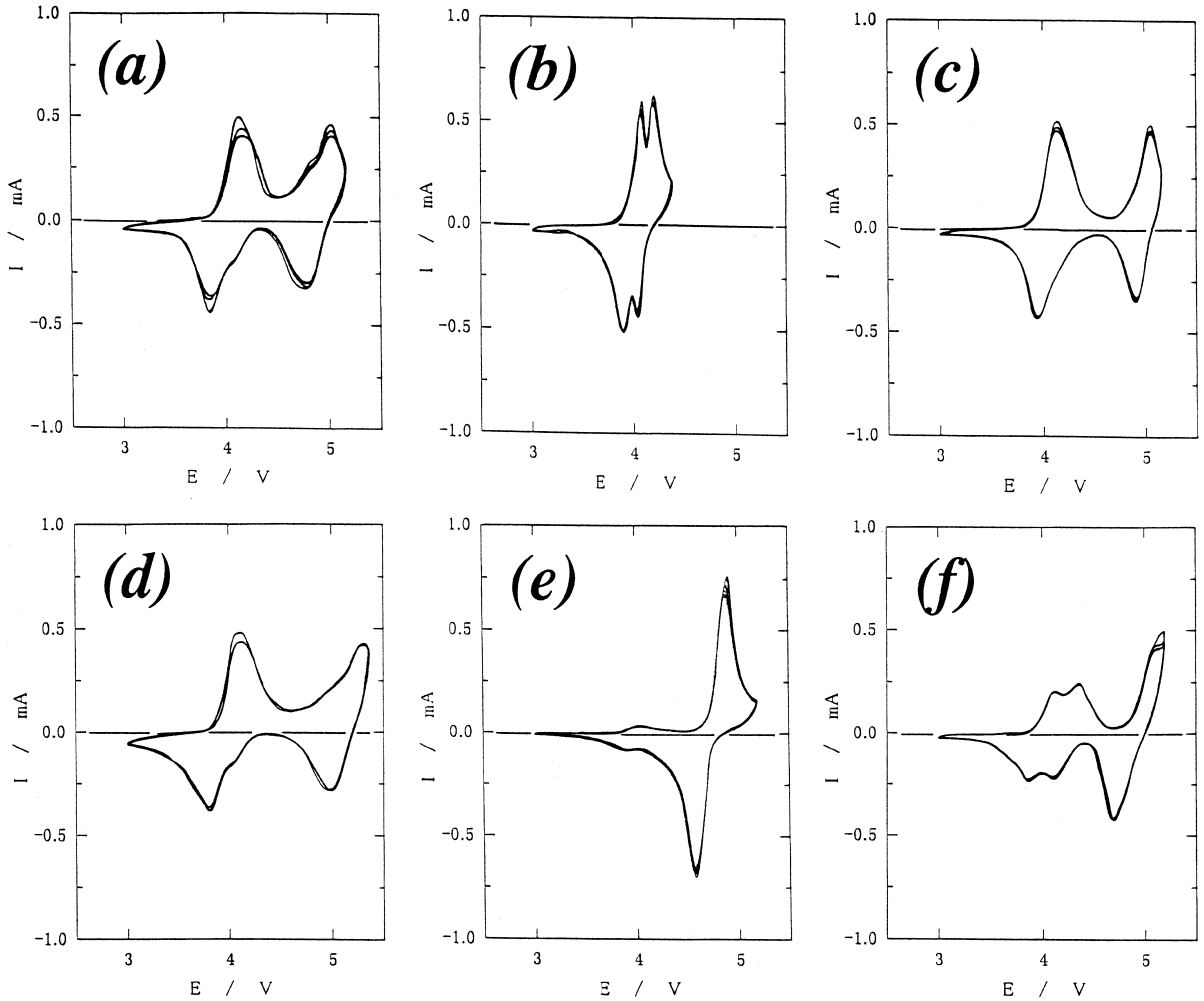

Fig. 2. Slow-scan voltammetry of $Li/Li[Me_{1/2}Mn_{3/2}]O_4$ cells (Me : (a) Cr, (b) Mn, (c) Fe, (d) Co, (e) Ni, or (f) Cu) at a rate of 0.2 mV s^{-1}. The electrolyte was 1 M $LiPF_6$ EC/DEC (1/1 by volume).

application of these materials to positive electrodes for lithium-ion batteries as follows:

$$Li[Me_{1/2}Mn_{3/2}]O_4 \Leftrightarrow \square_{1/2}Li_{1/2}[Me_{1/2}Mn_{3/2}]O_4 + (1/2)Li^+ + (1/2)e^- \text{ at about 4.0 V}$$

and $\square_{1/2}Li_{1/2}[Me_{1/2}Mn_{3/2}]O_4 \Leftrightarrow \square[Me_{1/2}Mn_{3/2}]O_4 + (1/2)Li^+ + (1/2)e^-$ at about 5.0 V for Me = Cr, Fe, Co, or Cu,

and $Li[Ni_{1/2}Mn_{3/2}]O_4 \Leftrightarrow \square[Ni_{1/2}Mn_{3/2}]O_4 + Li^+ + e^-$ at 4.8 V.

Table 1 lists structural and electrochemical parameters for these materials. One can make 5 V lithium-ion batteries with these materials combining with (natural) graphite [11], although stable electrolyte against both oxidation and reduction (0 to 5.5 V vs. Li^+/Li) is inevitably necessary for the implementation of such high-voltage lithium-ion batteries.

Self-assembled 3d-transition metal oxides or lithiated metal oxides of their own kind show clear relationship between operating voltage and d-electron character [12], i.e., 1.5–4.5 V against a lithium electrode. A series of $Li[Me_{1/2}Mn_{3/2}]O_4$, however, does not show such characters. Fig. 4 shows the levels of solid-state redox potentials for $Li[Me_{1/2}Mn_{3/2}]O_4$. The solid-state redox potentials were estimated from the mid-points voltages between respective oxidation and reduction peaks in the slow-scan voltammetry, which will be refined by using a concept of the electrochemical density of state [13]. As can be seen in Fig. 4, almost every sample shows discrete voltage at 4.0 ± 0.1 V and 5.0 ± 0.2 V which are independent of a kind of 3d-transition metal ions Me in $Li[Me_{1/2}Mn_{3/2}]O_4$. Single phase of $Li[V_{1/2}Mn_{3/2}]O_4$ is not succeeded yet to prepare, so that solid-state redox potential is still unknown. $Li[Zn_{1/2}Mn_{3/2}]O_4$ was examined carefully, but redox signal is not confirmed in voltages 3.5–5.3 V vs. Li^+/Li.

We are very interested in the effective use of iron and manganese in batteries, in addition to theoretical aspects of solid-state redox potentials of lithium insertion electrodes. According to the formulation described above for $Li[Fe_{1/2}Mn_{3/2}]O_4$, a total of 148 mAh g^{-1} of recharge-

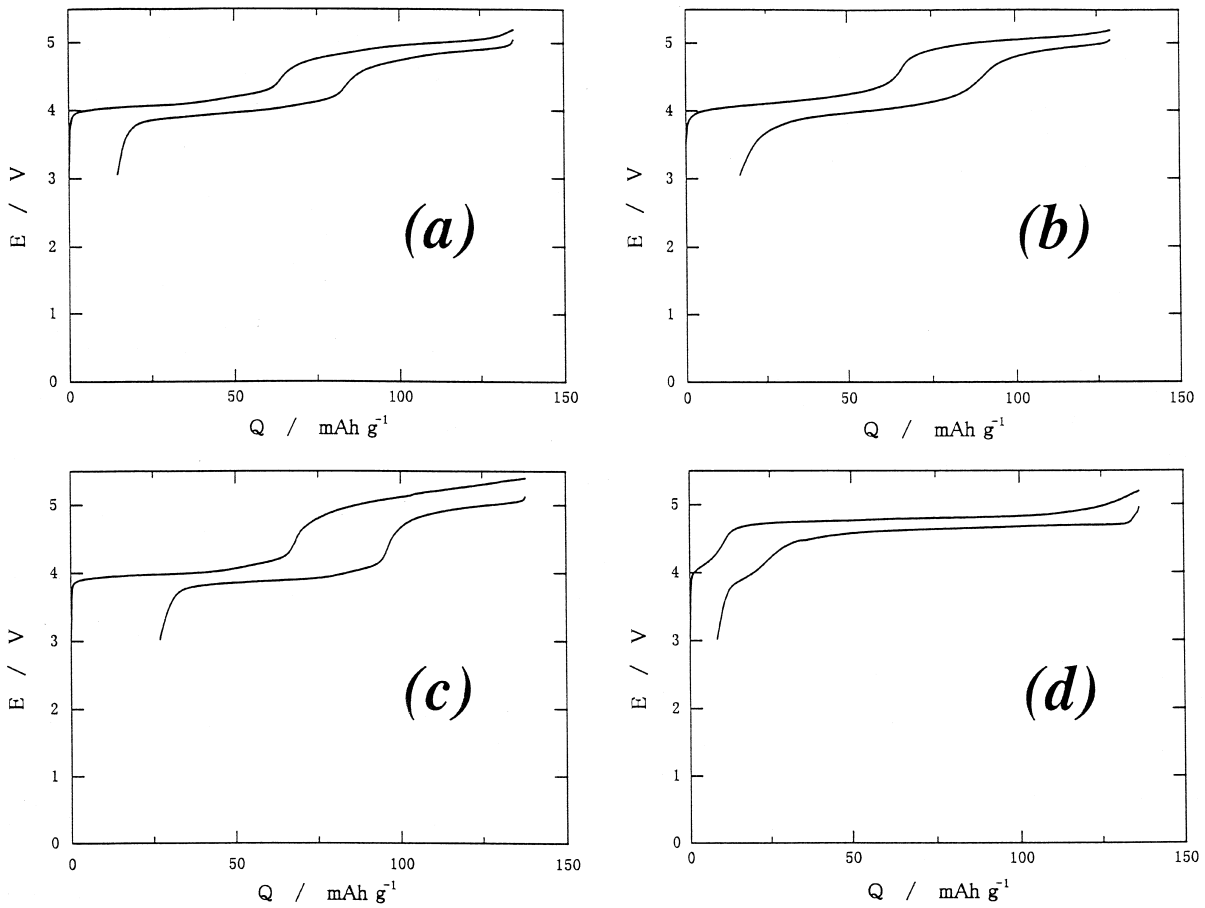

Fig. 3. Charge and discharge curves of (a) Li/Li[$Cr_{1/2}Mn_{3/2}$]O_4, (b) Li/Li[$Fe_{1/2}Mn_{3/2}$]O_4, (c) Li/Li[$Co_{1/2}Mn_{3/2}$]O_4, and (d) Li/Li[$Ni_{1/2}Mn_{3/2}$]O_4 cells operated in voltages above 3 V at a rate of 0.2 mA. Electrode area was 3 cm^2 (1.5 × 2.0 cm).

Table 1
Structural and electrochemical parameters for Li[$Me_{1/2}Mn_{3/2}$]O_4 (Me : 3d-transition metal)

Me in Li[$Me_{1/2}Mn_{3/2}$]O_4	Starting materials	Atmosphere	Lattice parameter (a/Å)	Oxygen positional parameter[a]	Theoretical capacities[b] (mAh · g^{-1})	
					3.5 < E < 4.5	4.5 < E
Ti	LiOH TiO_2(anatase) MnOOH(manganite)	N_2	8.33	0.263	–	–
V	–	–	–	–	–	–
Cr	LiOH Cr_2O_3 MnOOH(manganite)	Air	8.22	0.265	75	75
Mn	LiOH MnOOH(manganite)	Air	8.24	0.266	148	–
Fe	LiOH FeOOH(goethite) MnOOH(manganite)	Air	8.27	0.264	74	74
Co	LiOH $Co(OH)_2$ MnOOH(manganite)	Air	8.15	0.267	73	73
Ni	LiOH $Ni(OH)_2$ MnOOH(manganite)	O_2	8.19	0.267	?	147
Cu	LiOH CuO MnOOH(manganite)	O_2	8.21	0.269	72	72
Zn	LiOH $Zn(OH)_2$ MnOOH(manganite)	Air	8.22	–	–	–

[a]At the 32(e) sites in the space group Fd3m.
[b]Li[$Me_{1/2}Mn_{3/2}$]O_4 (Me = Cr, Mn, Fe, Co, Ni, or Cu) gives 144–150 mAh · g^{-1} of theoretical capacity as positive-electrode materials for lithium ion batteries.

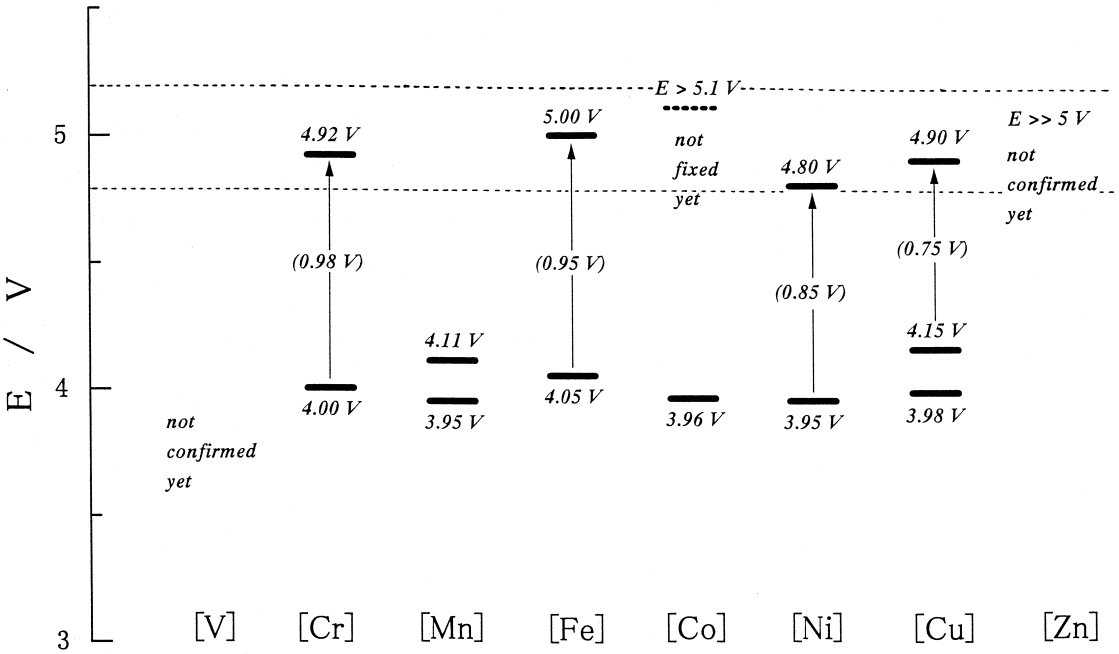

Fig. 4. Levels of solid-state redox potentials estimated by slow-scan voltammetry for $Li[Me_{1/2}Mn_{3/2}]O_4$. The chromium, iron, cobalt, nickel, or copper-containing sample having spinel-framework structures exhibits common solid-state redox potentials at 5.0 ± 0.2 V in addition to 4.0 ± 0.1 V vs. Li^+/Li.

able capacity (74 mAh g^{-1} at 4.0 V and 74 mAh g^{-1} at 5 V) is expected for the lithium-ion battery application. Increasing iron content results in a decrease of capacity at 4 V and an increase of capacity at 5 V. Such an optimization in terms of composition together with the design of test cells for constant-current charge–discharge cycles, and also the selection of electrolyte toward the implementation of 5 V lithium-ion batteries with (natural) graphite [11] using an organic electrolyte (as well as a 3.5 V solid-state lithium-ion battery with the zero-strain insertion material $Li[Li_{1/3}Ti_{5/3}]O_4$ [12,14] using a solid electrolyte) is under way in our laboratory.

In this paper, we have not stated specifically the valence states of the transition metal ions in the solid matrix [13]. For $Li[Fe_xMn_{2-x}]O_4$ ($0 < x < 1$) samples, Mossbauer spectral measurements will give a proper answer to this problem, and also the calculation of electronic structures of clusters, in which a target transition metal ion from Ti to Zn (initial state $+2$, $+3$, or $+4$), including the nearest-neighbor octahedrons consisting of a manganese ion (initial state $+3$ or $+4$) surrounded by six oxygen ions (starting state is -2) will give more insight into the solid-state redox reactions of lithium insertion materials using a discrete-variational (DV) X α method [15]. All results obtained from a series of experimental and theoretical works will be presented in the near future.

Acknowledgements

One of us (T.O.) wishes to thank Dr. D. Guyomard for his helpful discussion on the experimental techniques and also wishes to thank Dr. H. Komori and Mr. K. Furukawa, who were graduate students at Osaka City University during the academic years of 1989–1991 (H.K.) and 1992–1993 (K.F.), for their help in preparing and examining a series of samples in the early stage of this research. The present work was partially supported by grants in aid for Scientific Research from the Ministry of Education, Science, Sports and Culture, and Osaka City University Science Foundation.

References

[1] T. Ohzuku, S. Kitano, M. Iwanaga, H. Matsuno, A. Ueda, J. Power Sources 68 (1997) 646.
[2] G. Blasse, Phillips Res. Repts. Suppl. 3 (1) (1964) 121.
[3] T. Ohzuku, A. Ueda, M. Nagayama, J. Electrochem. Soc. 140 (1993) 1862.
[4] T. Ohzuku, K. Sawai, Denki Kagaku 64 (1996) 1060.
[5] T. Ohzuku, M. Kitagawa, T. Hirai, J. Electrochem. Soc. 137 (1990) 769.
[6] C. Sigala, D. Guyomard, A. Verbaere, Y. Piffard, M. Tournoux, Solid State Ionics 81 (1995) 162.
[7] Q. Zhong, A. Bonakdarpour, M. Zhang, Y. Gao, J.R. Dahn, J. Electrochem. Soc. 144 (1997) 205.
[8] Y. Ein-Eli, W.F. Howard Jr., J. Electrochem. Soc. 144 (1997) L205.
[9] Y. Ein-Eli, W.F. Howard Jr., S.H. Lu, S. Mukerjee, J. Mcbreen, J.T. Vaughey, M.M. Thackeray, J. Electrochem. Soc. 145 (1998) 1238.
[10] Y. Xia, M. Yoshio, J. Electrochem. Soc. 144 (1997) 4186.
[11] T. Ohzuku, Y. Iwakoshi, K. Sawai, J. Electrochem. Soc. 140 (1993) 2490.
[12] T. Ohzuku, A. Ueda, Solid State Ionics 69 (1994) 201.
[13] T. Ohzuku, A. Ueda, J. Electrochem. Soc. 144 (1997) 2780.
[14] T. Ohzuku, A. Ueda, N. Yamamoto, J. Electrochem. Soc. 142 (1995) 1431.
[15] H. Adachi, private communication.